

## Article

# Vesicular MicroRNA as Potential Biomarkers of Viral Rebound

Wilfried Wenceslas Bazié <sup>1,2,\*</sup> , Julien Boucher <sup>1</sup>, Isidore Tiandogo Traoré <sup>2,3</sup>, Dramane Kania <sup>2</sup>, Diane Yirgnur Somé <sup>2</sup>, Michel Alary <sup>4,5,6</sup>  and Caroline Gilbert <sup>1,7,\*</sup> 

<sup>1</sup> Axe de Recherche Maladies Infectieuses et Immunitaires, Centre de Recherche du CHU de Québec-Université Laval, Québec City, QC G1V 4G2, Canada; julien.boucher.2@ulaval.ca

<sup>2</sup> Programme de Recherche sur les Maladies Infectieuses, Centre Muraz, Institut National de Santé Publique, Bobo-Dioulasso 01 BP 390, Burkina Faso; tiandogo2002@yahoo.fr (I.T.T.); draka3703@yahoo.fr (D.K.); some.diane@yahoo.fr (D.Y.S.)

<sup>3</sup> Département de Santé Publique, Institut Supérieur des Sciences de la Santé, Université Nazi Boni, Bobo-Dioulasso 01 BP 1091, Burkina Faso

<sup>4</sup> Axe de Recherche Santé des Populations et Pratiques Optimales en Santé, Centre de Recherche du CHU de Québec-Université Laval, Québec City, QC G1S 4L8, Canada; michel.alary@crchudequebec.ulaval.ca

<sup>5</sup> Département de Médecine Sociale et Préventive, Faculté de Médecine, Université Laval, Québec City, QC G1V 0A6, Canada

<sup>6</sup> Institut National de Santé Publique du Québec, Québec City, QC G1V 5B3, Canada

<sup>7</sup> Département de Microbiologie-Infectiologie et d'Immunologie, Faculté de Médecine, Université Laval, Québec City, QC G1V 0A6, Canada

\* Correspondence: wilfried-wenceslas.bazie.1@ulaval.ca (W.W.B.); caroline.gilbert@crchudequebec.ulaval.ca (C.G.); Tel.: +1-(418)-525-4444 (ext. 44104) (W.W.B.); +1-(418)-525-4444 (ext. 46107) (C.G.); Fax: +1-(418)-654-2765 (C.G.)

**Abstract:** Changes in the cellular microRNA (miRNA) expression profile in response to HIV infection, replication or latency have been reported. Nevertheless, little is known concerning the abundance of miRNA in extracellular vesicles (EVs). In the search for a reliable predictor of viral rebound, we quantified the amount of miR-29a, miR-146a, and miR-155 in two types of plasma extracellular vesicles. Venous blood was collected from 235 ART-treated and ART-naive persons living with HIV (85 with ongoing viral replication,  $\geq 20$  copies/mL) and 60 HIV-negative participants at five HIV testing or treatment centers in Burkina Faso. Large and small plasma EVs were purified and counted, and mature miRNA miR-29a, miR-146a, and miR-155 were measured by RT-qPCR. Diagnostic performance of miRNA levels in large and small EVs was evaluated by a receiver operating characteristic curve analysis. The median duration of HIV infection was 36 months (IQR 14–117). The median duration of ART was 34 months (IQR 13–85). The virus was undetectable in 63.8% of these persons. In the others, viral load ranged from 108 to 33,978 copies/mL (median = 30,032). Large EVs were more abundant in viremic participants than aviremic. All three miRNAs were significantly more abundant in small EVs in persons with detectable HIV RNA, and their expression levels in copies per vesicle were a more reliable indicator of viral replication in ART-treated patients with low viremia (20–1000 copies/mL). HIV replication increased the production of large EVs more than small EVs. Combined with viral load measurement, quantifying EV-associated miRNA abundance relative to the number of vesicles provides a more reliable marker of the viral status. The expression level as copies per small vesicle could predict the viral rebound in ART-treated patients with undetectable viral loads.

**Keywords:** extracellular vesicles; HIV-1; viral replication; microRNA; miR-29a; miR-146a; miR-155; biomarker



**Citation:** Bazié, W.W.; Boucher, J.; Traoré, I.T.; Kania, D.; Somé, D.Y.; Alary, M.; Gilbert, C. Vesicular MicroRNA as Potential Biomarkers of Viral Rebound. *Cells* **2022**, *11*, 859. <https://doi.org/10.3390/cells11050859>

Academic Editor: Baharak Hosseinkhani

Received: 11 January 2022

Accepted: 24 February 2022

Published: 2 March 2022

**Publisher's Note:** MDPI stays neutral with regard to jurisdictional claims in published maps and institutional affiliations.



**Copyright:** © 2022 by the authors. Licensee MDPI, Basel, Switzerland. This article is an open access article distributed under the terms and conditions of the Creative Commons Attribution (CC BY) license (<https://creativecommons.org/licenses/by/4.0/>).

## 1. Introduction

Human immunodeficiency virus (HIV) causes a chronic infection characterized by reservoirs of latent retroviruses, making its eradication in the host very difficult [1]. Antiretroviral therapy (ART) suppresses virions replication, keeping it below detectable levels

or at a low level of viremia in conjunction with small numbers of infected cells [1–3]. Maintaining this suppression requires long-term adherence to ART with regular monitoring of viremia. In some patients, viral rebound occurs. It is defined as a persistent detectable level of HIV RNA arising in the blood after a period of suppression. Rebounds and persistent episodes of low-level detectable viremia are associated with a greater risk of subsequent virological failure, drug resistance, and impaired immune status [4–6].

In the absence of reliable early viral rebound indicators, various mathematical models and biomarkers have been studied as predictors of the time to viral rebound after interrupting ART [7,8]. While no strong evidence for any biomarker other than total HIV-1 DNA has been found, the persistence of low-level viremia has emerged as a factor in subsequent virological failure and is, therefore, a development that needs to be managed and prevented [9]. There is an urgent need to find a quantitative biomarker of viral rebound that is more accessible than total HIV-1 DNA and provides a better understanding of the mechanisms underlying viral rebound.

The discovery of secreted extracellular vesicles (EVs) and their role as intercellular messengers sheds new light on several physiological and pathological processes [10,11]. EVs are a heterogeneous group of circulating membranous bodies that vary in size and function, depending on their origin and biogenic pathway. They contain complex sets of functional molecules, including proteins, lipids, DNA, mRNA, and microRNA (miRNA) contents [10,11], which reflect the cell type of origin and suggest their investigation as a source of novel biomarkers in infectious diseases and cancer detection. Accumulating evidence suggests that miRNA expressed in EVs has diagnostic value as a liquid biopsy for diagnosis, prognosis, and monitoring several cancers [12–14]. Our previous studies have shown that, in patients living with HIV, large and small plasma EVs are loaded differentially with miRNA and may be helpful as biomarkers of immune activation [15,16].

At least one study suggests that HIV-1 modulates EV secretion through its negative regulatory factor (Nef) protein [17]. It was later demonstrated that, in cells infected with HIV-1 or human T lymphotropic virus type 1, the production of EVs containing viral materials precedes viral replication [18]. EVs can regulate the persistence and reactivation of HIV reservoirs through the deregulation of specific pathways that play a significant role in HIV replication [19,20].

Changes in cellular miRNA expression profiles in response to HIV infection have been reported [21]. The miRNA species involved in HIV infection can be divided into those that target HIV transcripts directly and those that affect the viral cycle through the regulation of host cellular factors [22]. Many miRNAs such as the miR-29 family and miR-155 have been associated with HIV replication and latency [23–25]. MiR-29a has been found very abundant in HIV-1-infected human T lymphocytes [23], and inhibiting it enhances HIV-1 viral production and infectivity, whereas the expression of miR-29 mimics suppresses viral replication. Differential expression between reactivated and latent cells has been observed for miR-155 and miR-146a, raising the possibility that specific miRNAs expressed abundantly in reactivated cells counter viral activation and perhaps promote a return to latency during transient virus production [25].

The idea that HIV replication modulates EV secretion and induces modification of cell miRNA expression led us to wonder if the EV miRNA content might predict viral rebound in patients on ART. In this article, we investigate the miR-29a, miR-146a, and miR-155 expression levels in large and small plasma EVs purified from HIV patients with and without viral replication and evaluate the potential of this measurement as a rapid clinical test for identifying viremic patients.

## 2. Materials and Methods

### 2.1. Study Subjects

HIV-infected participants were recruited by referral from five follow-up centers in Bobo-Dioulasso and Ouagadougou (Burkina Faso). These included the Yerelon clinics (Centre Muraz) of both towns, specialized in female sex worker follow-up, the Association

African Solidarité (AAS) center for the follow-up of men who have sex with men, and dedicated follow-up day hospital centers CHU Sourô Sanou (Bobo-Dioulasso) and CHU Yalgado Ouédraogo (Ouagadougou). The HIV-negative participants were recruited in the Yerelon clinics, which also offer HIV testing.

### 2.2. Quantitation of HIV-1 RNA, CD4 and CD8 T Lymphocytes

The HIV-1 viral load was measured using the COBAS® AmpliPrep /COBAS® TaqMan® Real-Time PCR assay (TaqMan, Roche Diagnostics, Mannheim, Germany), which targets two highly conserved regions of the HIV-1 genome and has a detection limit of 20 copies/mL.

Absolute counts of CD4+ T and CD8+ T lymphocytes were obtained using a BD FACSCount™ System flow cytometer (Becton Dickinson, San Jose, CA, USA).

### 2.3. Purification of Extracellular Vesicles

Purification of EVs was performed as described previously [15,16]. Briefly, blood obtained by venipuncture with citrate as an anticoagulant was centrifuged for 10 min at  $400\times g$  at room temperature. The plasma was centrifuged for 10 min at  $3000\times g$  to obtain platelet-free-plasma and stored at  $-80\text{ }^{\circ}\text{C}$  until analysis. Thawed platelet-free plasma (250  $\mu\text{L}$ ) was treated with proteinase K (1.25 mg/mL, Ambion™, Thermo Fisher Scientific, Waltham, MA, USA) for 10 min at  $37\text{ }^{\circ}\text{C}$ . This pretreatment of plasma with proteinase K is described to critically reduce the amount of non-EV proteins (albumin and the apolipoproteins A-1 and B), which can be co-purified with EV. This digestion step destroys proteins and their cargo (mRNA and miRNA), and they were removed with the washing step. Large EVs were purified by centrifuging proteinase-K-pretreated plasma for 30 min at  $17,000\times g$  at room temperature. The supernatant was mixed with 63  $\mu\text{L}$  of ExoQuick-TC™ (SBI via Cedarlane, Burlington, ON, Canada) in an Eppendorf tube and maintained at  $4\text{ }^{\circ}\text{C}$  overnight. The large EV pellet was resuspended in 250  $\mu\text{L}$  of microfiltered (0.22- $\mu\text{m}$  pore size membrane) 1x phosphate-buffered saline (WISENT Bioproducts, Saint-Jean-Baptiste, QC, Canada) and centrifuged for 30 min at  $17,000\times g$ . The supernatant was discarded, and the washed large EV pellet was resuspended in 250  $\mu\text{L}$  of PBS and kept at  $4\text{ }^{\circ}\text{C}$ . Small EVs were obtained from the ExoQuick-TC™ precipitation after centrifuging for 30 min at  $1500\times g$ . The ExoQuick precipitate was centrifuged for 30 min at  $1500\times g$ . The supernatant was discarded, and the pellet was washed in PBS and centrifuged for 5 min at  $1500\times g$  to obtain small EVs, which were resuspended in 250  $\mu\text{L}$  of PBS by vortex mixing and kept at  $4\text{ }^{\circ}\text{C}$ . The size of the EV was determined by hydrodynamic radius measurements using a Zetasizer Nano S (Malvern Instruments, Ltd., Malvern, United Kingdom). This technique is based on the light scattering intensity due to the Brownian motion of EVs, characterized by a diffusion constant [26]. The size distribution is obtained from the distribution of diffusion constants using the Einstein–Stokes equation [26]. The measurements were made at a fixed position with an automatic attenuator and at a controlled temperature. One hundred microliters of EV suspension were used for each sample, and two measurements were averaged. We have submitted all relevant data of our experiments to the EV-TRACK knowledgebase (EV-TRACK ID: EV220124) [27].

### 2.4. EV Flow Cytometry Analysis

Purified EVs were stained with the lipophilic fluorescent carbocyanine dye DiD (DiI18(5) solid: 1,1'-dioctadecyl-3,3',3'-tetramethylindodicarbocyanine 4-chlorobenzene-sulfonate salt (Invitrogen™, Carlsbad, CA, USA), and the vesicular or cell-permeable dye CFSE (carboxyfluorescein diacetate succinimidyl ester, Invitrogen™, Carlsbad, CA, USA). DiD and CFSE were prediluted, respectively, 1/100 and 1/500 with filtered (0.22  $\mu\text{m}$ ) PBS 1X + EDTA (100  $\mu\text{M}$  for the final concentration). Forty microliters of DiD diluted solution (final dilution 1/200, 1  $\mu\text{g}/\text{mL}$ ) was added to 10  $\mu\text{L}$  of EV suspension. After 5 min at  $37\text{ }^{\circ}\text{C}$ , 50  $\mu\text{L}$  of CFSE (diluted 1/1000, 1  $\mu\text{g}/\text{mL}$ ) were added. After 15 min ( $37\text{ }^{\circ}\text{C}$ ), the

staining was fixed by adding 0.02% Pluronic F-127 (Invitrogen™, Carlsbad, CA, USA) solution. Next, 100 µL of 4% paraformaldehyde (Fisher scientific™, Ottawa, CA, USA) solution was added and incubated for 20 min, and the tube was completed to 400 µL with 200 µL of filtered PBS 1X. Then, 5 µL of 15-µm count beads (Polybead® Microspheres 15 µm, Polysciences, Inc., Warrington, PA, USA) were mixed in by vortex. A flow cytometry method described previously [15,16] was used to count EVs in a FACS Canto II Special Order Research Product cytofluorometer equipped with forward scatter coupled to a photomultiplier tube (FSC-PMT) with the “small particles option” (BD Biosciences, Franklin Lakes, NJ, USA). Gating strategies for EV identification and analysis are described elsewhere [16].

### 2.5. MicroRNA Quantification

EV suspension (100 µL) was diluted 3:1 in TRIzol LS (Ambion™, Life Technologies, Carlsbad, CA, USA) and maintained at −80 °C. Total RNA was extracted, mixed with 10 µL of diethylpyrocarbonate water, and quantified in 1 µL using a BioDrop-µLITE kit (Isogen Life Science, Utrecht, The Netherlands). After treatment with RNase-free DNase I (Ambion™ Life Technologies), 100 ng of RNA was reverse-transcribed using a HiFlex miScript RT II kit according to the manufacturer’s instructions (Qiagen, Hilden, Germany). Mature miR-29a (#MS00003262), miR-146a-5p (#MS00006566), and miR-155-5p (#MS00031486) were detected by quantitative polymerase chain reaction (RT-qPCR) using an miScript primer assay kit and miScript SYBR Green PCR kit (Qiagen). Mature microRNA as cDNA was amplified in a CFX384 Touch Real-Time PCR Detection System (Bio-Rad, Hercules, CA, USA) using 40 cycles of 94 °C for 15 s, 55 °C for 30 s, and 72 °C for 30 s. Reaction specificity was confirmed using the melt curve procedure (65–95 °C, 0.5 °C per 5 s) at the end of the amplification protocol according to the manufacturer’s instructions. A microRNA control (miRTC control # MS00000001) was used in conjunction with the miScript II RT Kit to ensure the quality of the reverse transcription during the qPCR step. A standard curve was used for the absolute quantification of microRNA. Quantifying miRNA was expressed as copies per µg of RNA and copies per vesicle, as described previously [15].

### 2.6. Transmission Electron Microscopy

Briefly, large and small EV pellets purified as described above were suspended with glutaraldehyde 2.5% (Sigma-Aldrich, St. Louis, MO, USA) in 0.1-M sodium cacodylate (Sigma-Aldrich, St. Louis, MO, USA) buffer, pH 7.4. Ten microliters of the EV sample were pipetted onto a nickel grid with carbon-coated formvar film and incubated for 10 min. Excess liquid was removed by blotting. The grids were stained for 2 min with 2% uranyl acetate solution. Images were acquired using a FEI Tecnai Spirit G2 (FEI, Eindhoven, The Netherlands) transmission electron microscope equipped with a bottom-mounted CCD camera at 80 kV.

### 2.7. Statistical Analysis

All analyses were performed with GraphPad Prism 8 (GraphPad Inc, San Diego, CA, USA) and RStudio Version 1.4.1103 (Integrated Development for R. RStudio, PBC, Boston, MA, USA, 2020, <http://www.rstudio.com/>) to build correlation matrices and principal component analyses. Participant demographic and clinical characteristics were presented as a proportion or median with an interquartile range (IQR) and tabulated (Tables 1 and S1). Initial tests of normality and log normality indicated that the EV count and miRNA content expressed as copies/µg and copies/vesicle both fit a lognormal distribution. All values were therefore transformed to logarithms. Data were then analyzed assuming a Gaussian distribution using parametric tests, and ordinary one-way ANOVA corrected for multiple comparisons using the Tukey test for three or more group comparisons. In all graphs, the results are presented as the geometric mean with geometric standard deviation factor. Pearson parametric correlation tests were performed to build correlation matrices in R. The diagnostic value of the EV miRNA content was evaluated using receiver operating charac-

teristic (ROC) curves. Analyses were performed using the Wilson/Brown method, and the results were tabulated. A *p*-value less than 0.05 was considered statistically significant.

**Table 1.** Demographic and clinical characteristics of the study participants.

	Control ( <i>n</i> = 60)	HIV+ ( <i>n</i> = 235)	<i>p</i> -Value	HIV+		HIV+ Viral Load Detectable			
				Viremic ( <i>n</i> = 85)	ART > 6 Months, Viral Load Undetectable ( <i>n</i> = 128)	<i>p</i> -Value	ART-Naïve ( <i>n</i> = 17)	ART-Treated ( <i>n</i> = 68)	<i>p</i> -Value
Male, <i>n</i> (%)	14 (23.3)	68 (28.9)	0.3880	28 (32.9)	31 (24.2)	0.1636	6 (35.3)	22 (32.4)	0.8175
Female sex workers: <i>n</i> (%)		96 (40.9)		30 (35.3)	63 (49.2)	0.1208	2 (11.8)	28 (41.2)	0.0536
Men who have sex with men: <i>n</i> (%)		40 (17.0)		19 (22.3)	20 (15.6)		4 (23.5)	15 (22.1)	
Age (y)	27 (22–32)	36 (30–44)	<0.0001	35 (30–42)	38 (32–45)	0.0553	37 (27–4)	35 (30–42)	0.9577
<20	3 (5.0)	5 (2.1)		2 (2.4)	2 (1.6)		1 (5.9)	1 (1.5)	
20–29	34 (56.7)	37 (15.7)		17 (20.0)	16 (12.5)		4 (23.5)	13 (19.1)	
30–39	19 (31.7)	94 (40.0)	<0.0001	37 (43.5)	49 (38.3)	0.2670	5 (29.4)	32 (47.0)	0.4993
40–49	4 (6.6)	70 (29.8)		20 (23.5)	47 (36.7)		5 (29.4)	15 (22.1)	
≥ 50		29 (12.3)		9 (10.6)	14 (10.9)		2 (11.8)	7 (10.3)	
HIV duration (month)	NA	36 (14–117)		31 (8–72)	55 (24–120)	0.0313	8 (1–72)	36 (12–72)	0.9891
CD4 T cells/μL	992 (794–1276)	466 (330–696)	<0.0001	382 (213–561)	513 (386–755)	<0.0001	583 (318–742)	354 (188–507)	0.0860
CD8 T cells/μL	584 (447–715)	770 (543–1089)	<0.0001	841 (573–1049)	736 (536–1093)	0.6081	794 (570–1036)	848 (544–1016)	0.7852
CD4/CD8	1.8 (1.4–2.1)	0.6 (0.4–1.0)	<0.0001	0.5 (0.3–0.8)	0.7 (0.5–1.0)	<0.0001	0.6 (0.4–1.0)	0.4 (0.3–0.7)	0.0185
ART, <i>n</i> (%)	NA	206 (87.7%)		68 (80.0%)	NA		NA	NA	
ART duration (month)	NA	34 (13–85)		24 (8–62)	38 (21–96)	0.0231	NA	24 (8–62)	
Undetectable HIV viral load (<20 copies/mL), <i>n</i> (%)	NA	150 (63.8)		NA	NA		NA	NA	
HIV-1 viral load (copies/mL)	NA	30,032 (108–33,978)		30,032 (108–33,978)	NA		17,330 (3,032–39,416)	1446 (82–24,578)	0.2958

Ranges indicated are interquartile (IQR); NA = not applicable; CD4 and CD8 counts are in cells per μL, HIV and ART refer to human immunodeficiency virus and antiretroviral therapy status.

### 3. Results

#### 3.1. HIV-1 Replication Could Be Induces the Production of Large EVs

HIV-1 replication in vitro induces the production of EVs [28], and heterogeneous EV populations found in plasma from ART-naïve people living with HIV (PLWH) are more abundant than in successfully treated ART patients [29]. This study focused on two categories of EVs, called large and small (Figure S1). The demographic and clinical characteristics of the participants are summarized in Table 1 and Table S1. The median age was 36 years (IQR 30–44) in the HIV+ group (*n* = 235) and 27 years (IQR 22–32) among the uninfected participants (control, *n* = 60). The median CD4 T cell counts were, respectively for the control and HIV+ group, 992 (IQR 794–1276) and 466 (IQR 330–696) per μL, and the median CD8 T cell counts were 584 (IQR 447–715) and 770 (IQR 543–1089) per μL, giving median CD4/CD8 ratios of 1.8 (IQR 1.4–2.1) and 0.6 (IQR 0.4–1.0). In PLWH participants, 40.9% were female sex workers, and 17.0% were men who have sex with men. The median duration of HIV infection was 36 months (IQR 14–117), and 87.7% of HIV+ participants were ART-treated for 34 months (IQR 13–85). HIV-1 RNA was undetectable (viral load < 20 copies/mL) in 63.8% of these persons, and the median detectable viremic load was 30,032 copies/mL (IQR 108–33,978). Participants' HIV status, ART use, and viral load are summarized in Figure 1A.

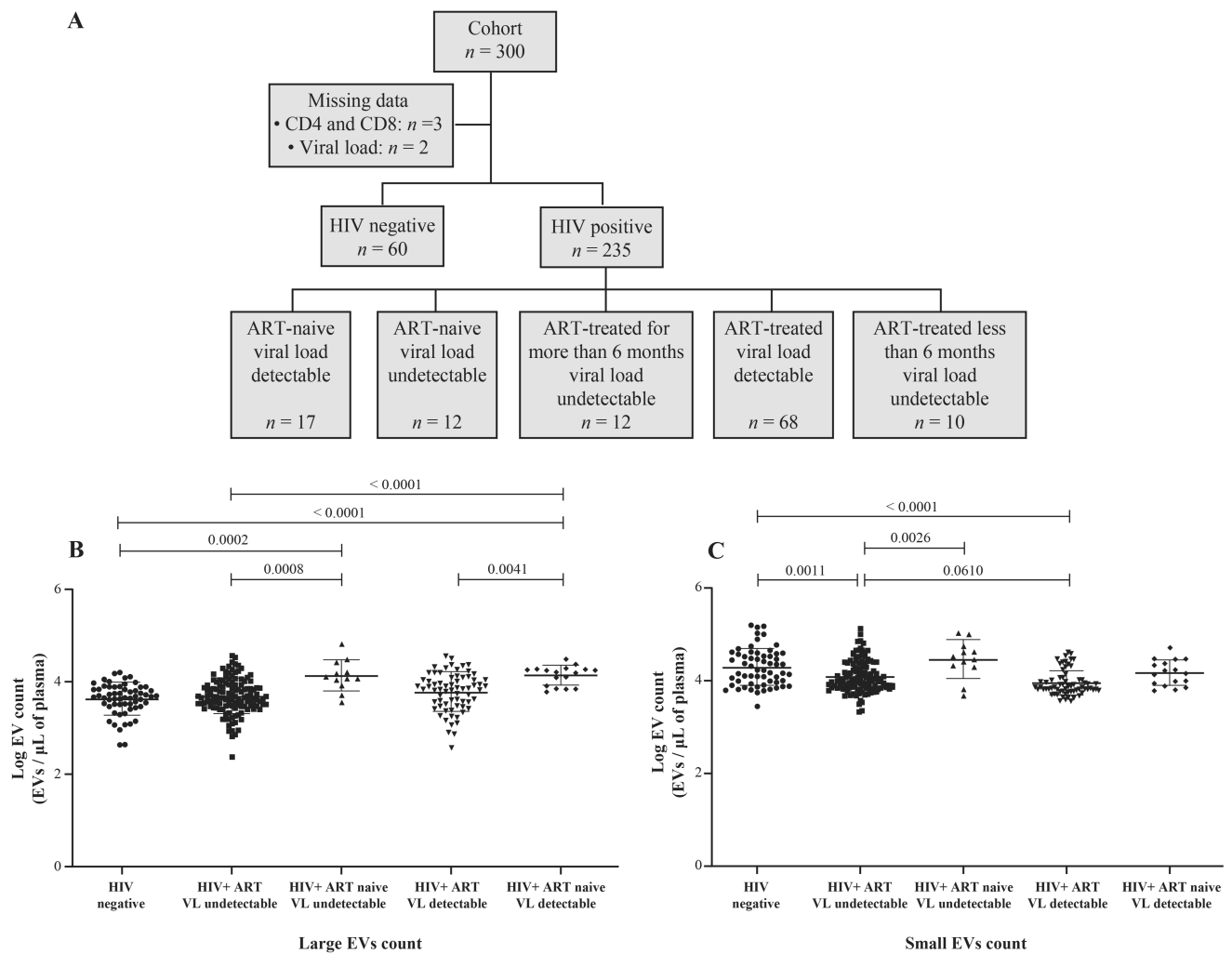


**Figure 1.** Flow chart of study participant categorization (A). Counts of purified large (B) and small (C) plasma EVs by flow cytometry using DID and CFSE staining. Study participants were HIV-negative, HIV-positive on antiretroviral therapy (ART) for more than six months, or HIV-positive and ART-naive, with an undetectable or detectable viral load (VL). An ordinary one-way ANOVA corrected for multiple comparisons using the Tukey test was used to compare groups.

Our previous observations of small EVs being the more abundant category in plasma [15,16] are corroborated (Figure 1B,C). EVs are overall more abundant in ART-naive viremic or non-viremic participants than in the corresponding ART-treated patients (Figures 1B,C and S2B,C). A significant difference in small EV abundance is noted between viremic ART patients and nonviremic (successfully treated) ART patients (Figure S2C). These results show that large plasma EVs accumulate during HIV-1 replication and that ART decreases EV abundance. More importantly, small EV abundance decreases significantly during ART in viremic patients with over 1000 copies/mL.

### 3.2. MicroRNA Content of Large versus Small EVs

In previous studies using peripheral blood mononuclear cells, the concentration of miR-29a was found inversely correlated with viremia, and its overexpression has been associated with the inhibition of viral replication and thus appears to force HIV-1 into latency [23,24,30]. Comparing nonviremic HIV+ patients relative to the control (HIV-) participants, we found no significant difference in miR-29a expressed as copies per  $\mu\text{g}$  RNA or copies per large vesicle (Figure 2A,C). In contrast, miR-29a copies per  $\mu\text{g}$  RNA were increased significantly in small EVs of viremic patients compared to the control group

(Figure 2B), as were copies per vesicle (Figure 2D). In addition, copies per vesicle were significantly increased in viremic compared to nonviremic ART-treated patients (Figure 2D). This latter comparison held properly over different levels of viremia (Figure S3D). These data show altogether that HIV-1 replication during ART induces the overexpression of miR-29a in small plasma EVs.

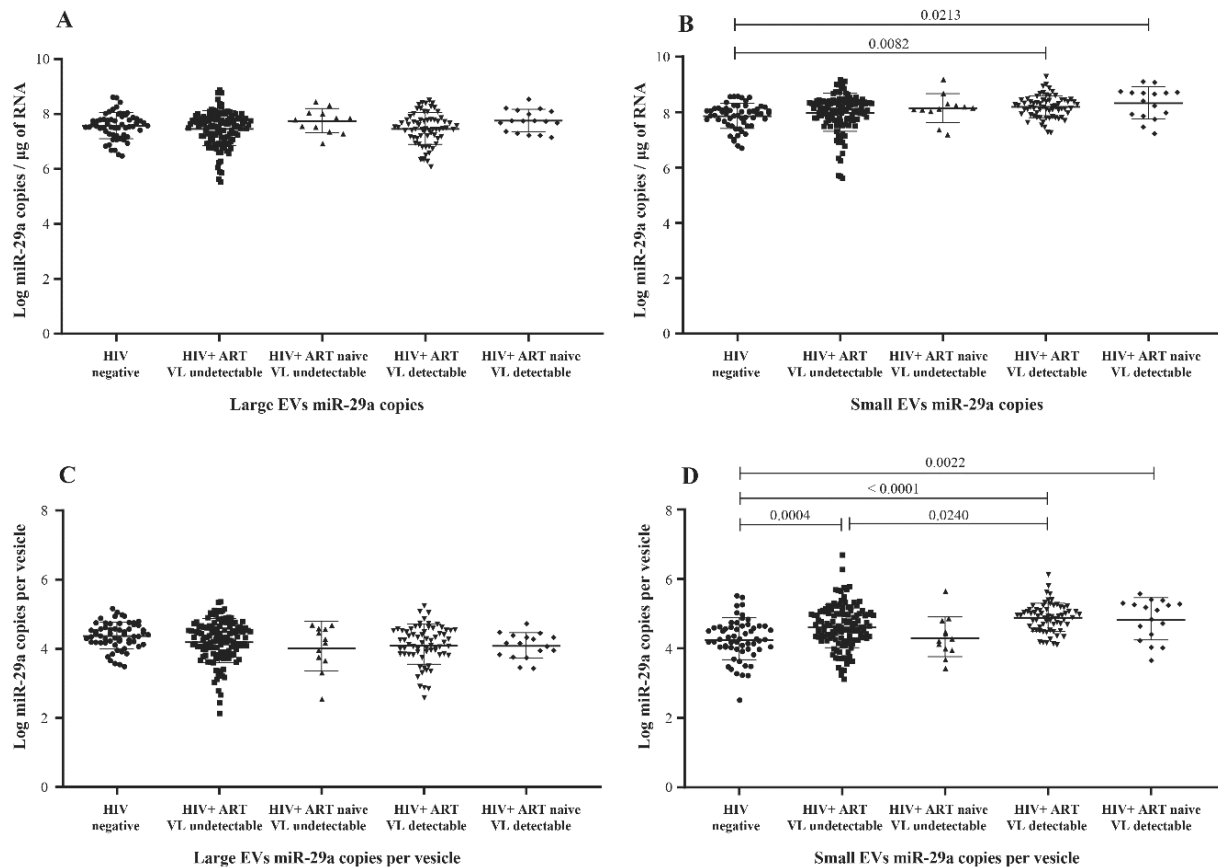


**Figure 2.** Mature miR-29a content expressed as copies per  $\mu\text{g}$  of total RNA in large (A) and small (B) plasma EVs and expressed as copies per large vesicle (C) and copies per small vesicle (D). See the flow chart in Figure 1 for study participant group descriptions. Values are log<sub>10</sub>-transformed. An ordinary one-way ANOVA was used with the Tukey test for between-group multiple comparisons.

MicroRNA 146a production is an established marker of inflammation [30,31], a significant concern in managing HIV infection. Copies of miR-146a in large and small plasma EVs were more abundant in HIV+ participants than in the control group (Figure 3A,B) and more abundant in viremic than nonviremic persons when small EVs are compared (Figure 3B,D), especially when the viral load is at least 1000 copies per mL (Figure S4B,D). ART was associated with a significant decrease in miR-146a in large and small EVs (Figure 3A,B). These results show that miR-146a increases in plasma EVs of HIV+ patients and that viral replication could be potentiating this response in small EVs.

Previous studies have shown elevated levels of miR-155 in plasma, peripheral blood mononuclear cells, CD4 T and CD8 T cells, and EVs from HIV-1-infected patients [29,32–34]. Here, we compared its copy numbers in large and small plasma EVs purified from viremic and nonviremic HIV+ patients, as well as uninfected persons. Unlike miR-29a and miR-146a, miR-155 copies per  $\mu\text{g}$  of RNA were more abundant in large EVs from ART-naive nonviremic-infected patients, even compared to the ART-treated group (Figure 4A). Its expression in large and small vesicles does not appear to be proportionate to viremia (Figure S5A,B). Copies per large vesicle were decreased in viremic patients compared to control participants (Figures 4C and S5C), whereas copies per small vesicles varied among

the participant groups (Figure 4D) but were not proportionate to viremia (Figure S5D). These results nevertheless showed patterns of the differential expression of miR-155 in large and small EVs associated with viremia.

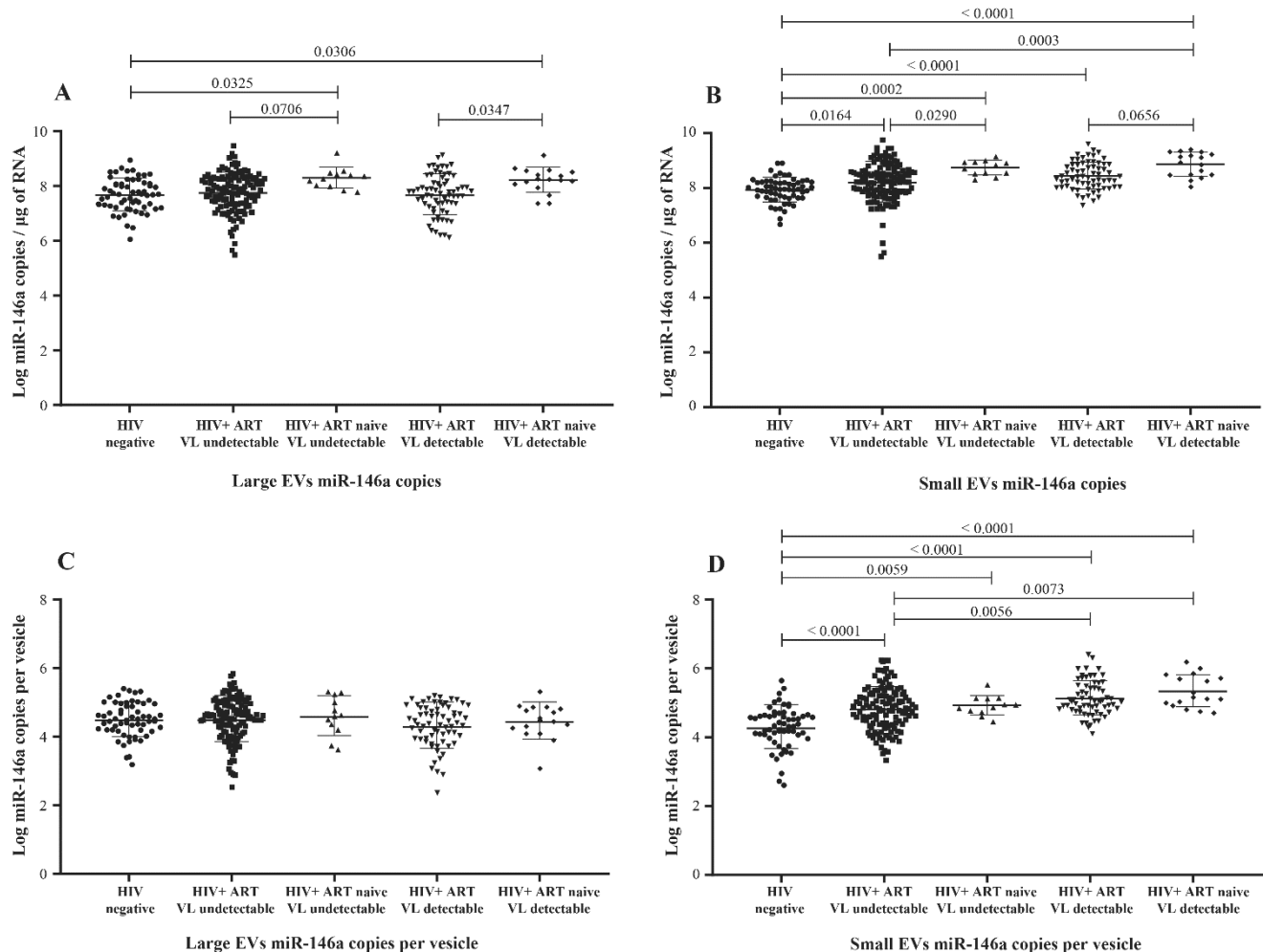


**Figure 3.** Mature miR-146a content expressed as copies per  $\mu\text{g}$  of total RNA in large (A) and small (B) plasma EVs and expressed as copies per large vesicle (C) and copies per small vesicle (D). See the flow chart in Figure 1 for study participant group descriptions. Values are log<sub>10</sub>-transformed. An ordinary one-way ANOVA was used with the Tukey test for between-group multiple comparisons.

### 3.3. Correlation between EV MicroRNA Content and Demographic/Clinical Parameters

Correlograms (Figures 5 and S6) summarize the relationships between our measurements. MiR-155 copies per  $\mu\text{g}$  RNA or large EV were correlated significantly and inversely with viral load over 1000 copies per mL of ART-naive (Figures 5A and S6B). In contrast, miR-29a and miR-146a copies in small EVs were positively correlated with the viral load in ART patients with over 1000 viral copies/mL (Figure S6C). An inverse correlation between age and miR-146a expression in small EVs was observed. As expected, the HIV-1 viral load was correlated inversely with the CD4 T-cell count and CD4/CD8 ratio (Figure 5). The number of small EVs was positively correlated with the CD4 T-cell count and negatively with the viral load in ART-naive patients (Figure 5A). Although the correlation between miRNA content and viral load appears to be strong, a significant discriminator between the viremic status groups remains identified.

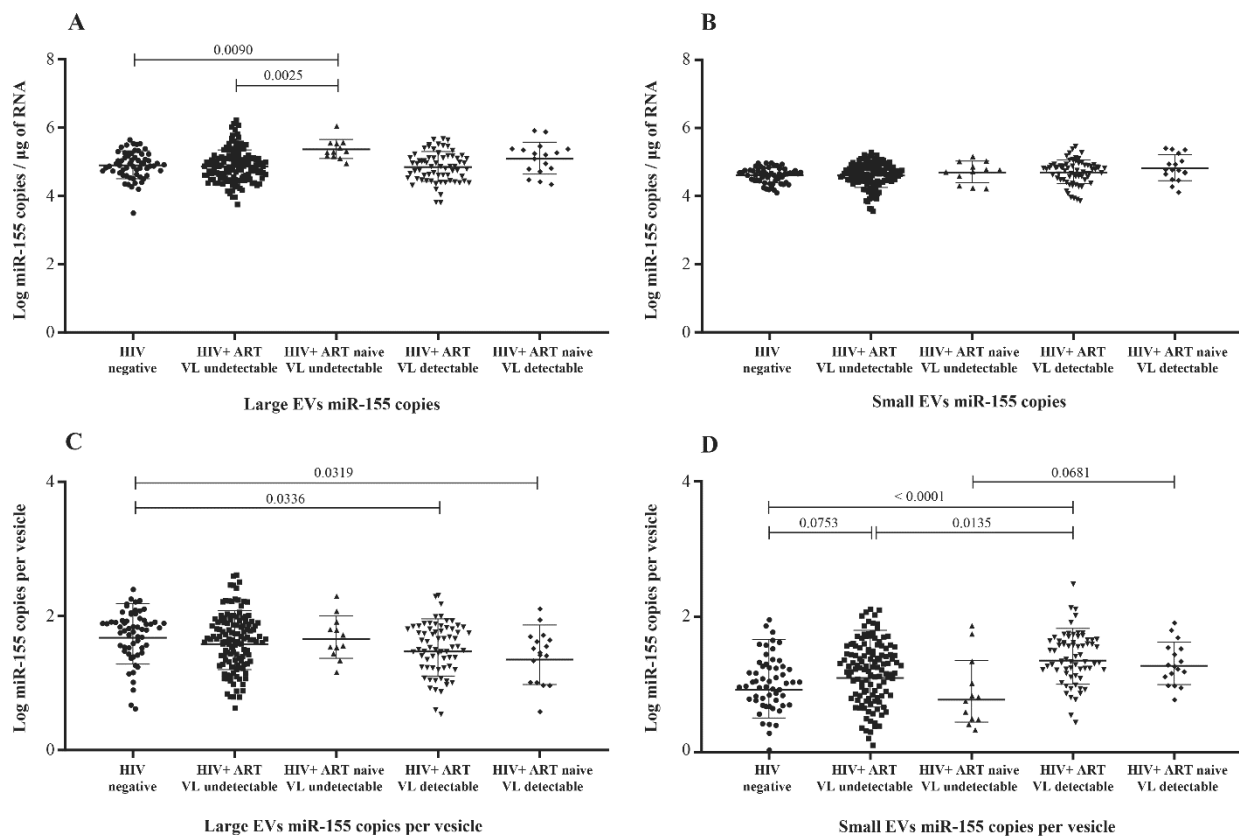


**Figure 4.** Mature miR-155 content expressed as copies per µg of total RNA in large (A) and small (B) plasma EVs and expressed as copies per large vesicle (C) and copies per small vesicle (D). See the flow chart in Figure 1 for the study participant group descriptions. Values are log<sub>10</sub>-transformed. An ordinary one-way ANOVA was used with the Tukey test for between-group multiple comparisons.

### 3.4. Principal Component Analysis of the EV Measurement/Viral Replication Association

Given our correlogram results (Figures 5 and S6) showing several correlations between the miRNA contents of large and small EVs and the clinical status, we used a principal component analysis to discriminate between the five patient groups (Figure 1A) based on miRNA copies per µg of the total RNA and copies per vesicle (Figure 6). The levels of miR-29a (Figure 6A,B), miR-146a (Figure 6C,D), and miR-155 (Figure 6E,F) each clearly distinguished between HIV- and viremic HIV+ individuals. The strength of this measurement is apparent in the confidence ellipses and the mean coordinates of the individuals in each group. Copies per vesicle seem to give a better graphical representation of the individuals, showing more excellent proximity of the viremic (ART-treated and ART-naïve) and nonviremic (ART-treated and ART-naïve) group mean points. These results suggest that the quantitative measurement of EV-associated miR-29a, miR-146a, and miR-155 might be helpful for the diagnosis of individual viral statuses.

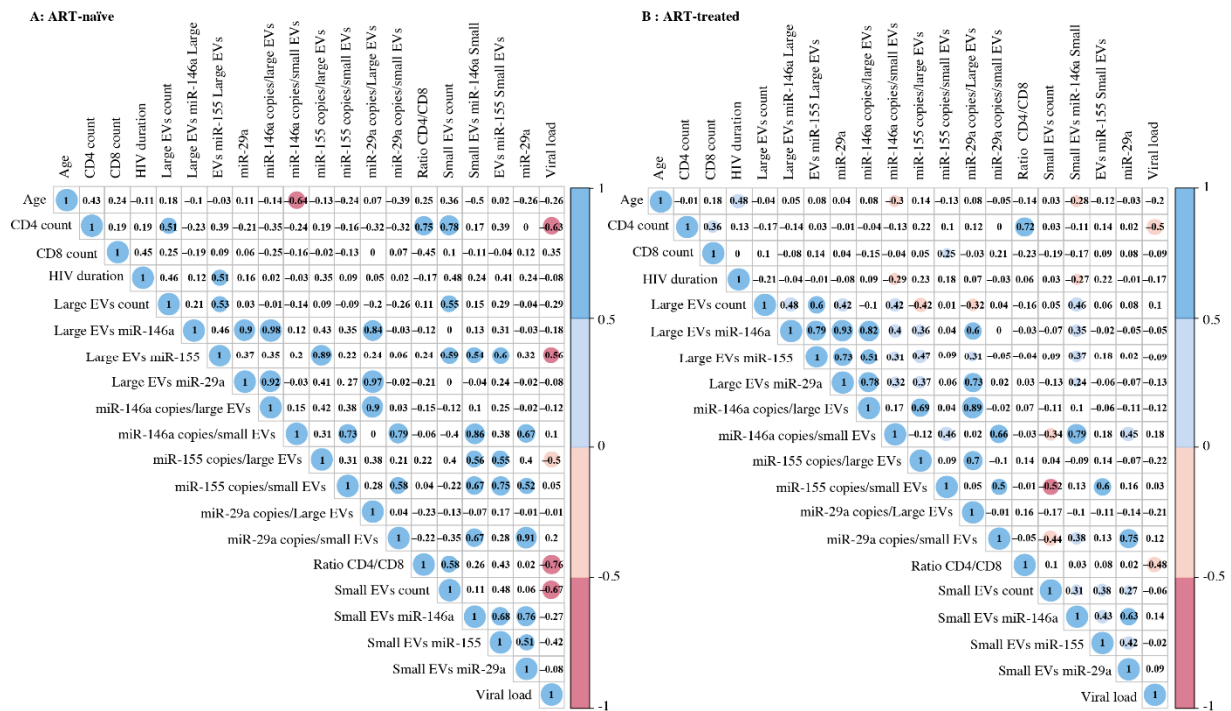


**Figure 5.** Correlation matrix between the different variables of ART-naïve (A) or ART-treated (B) study participants with viremia. The sizes and colors of the circles indicate the strength of the correlation, and the colored boxes indicate significant correlation at the threshold of 0.05. A two-tailed Pearson correlational test was computed between variables.

*3.5. MicroRNA 29a, 146a, and 155 Copies per Small EV and Mir-155 Copies in Large EV as Potential Biomarkers of Viral Rebound*

Tables 2 and S2–S7 show receiver operator characteristic areas under the curve for the predictability of HIV-1 viral rebound based on the EV miRNA content using HIV-negative participants as the control group (Table 2 left column, and Tables S2 and S5), then nonviremic ART-naïve patients (Table 2 middle column, and Tables S3 and S6), and finally, nonviremic patients ART-treated for more than six months and having a CD8 T cell count < 500 cells/ $\mu$ L and CD4 T cell count  $\geq$  500 cells/ $\mu$ L (reference patient) (Table 2 right column, and Tables S4 and S7). Using the reference patient as a control group, miR-29a, miR 146a, and miR155 copies per small EVs (Figure 7) and miR-155 copies in large EVs (Figure 8) discriminated viremic patients. In addition, for low-viremic ART-treated patients (20–1000 copies/mL) and in subgroups of viremic participants (female sex workers, men who have sex with men, and men and women from the general population), miR-29a, miR 146a, and miR-155 copies per small EVs remain the best discriminators of viremic patients (Tables S2–S7). These results confirm that the three miRNA species expressed as copies per vesicle distinguish viremic patients and, more importantly, are the best discriminator of ART-treated low-viremic patients.

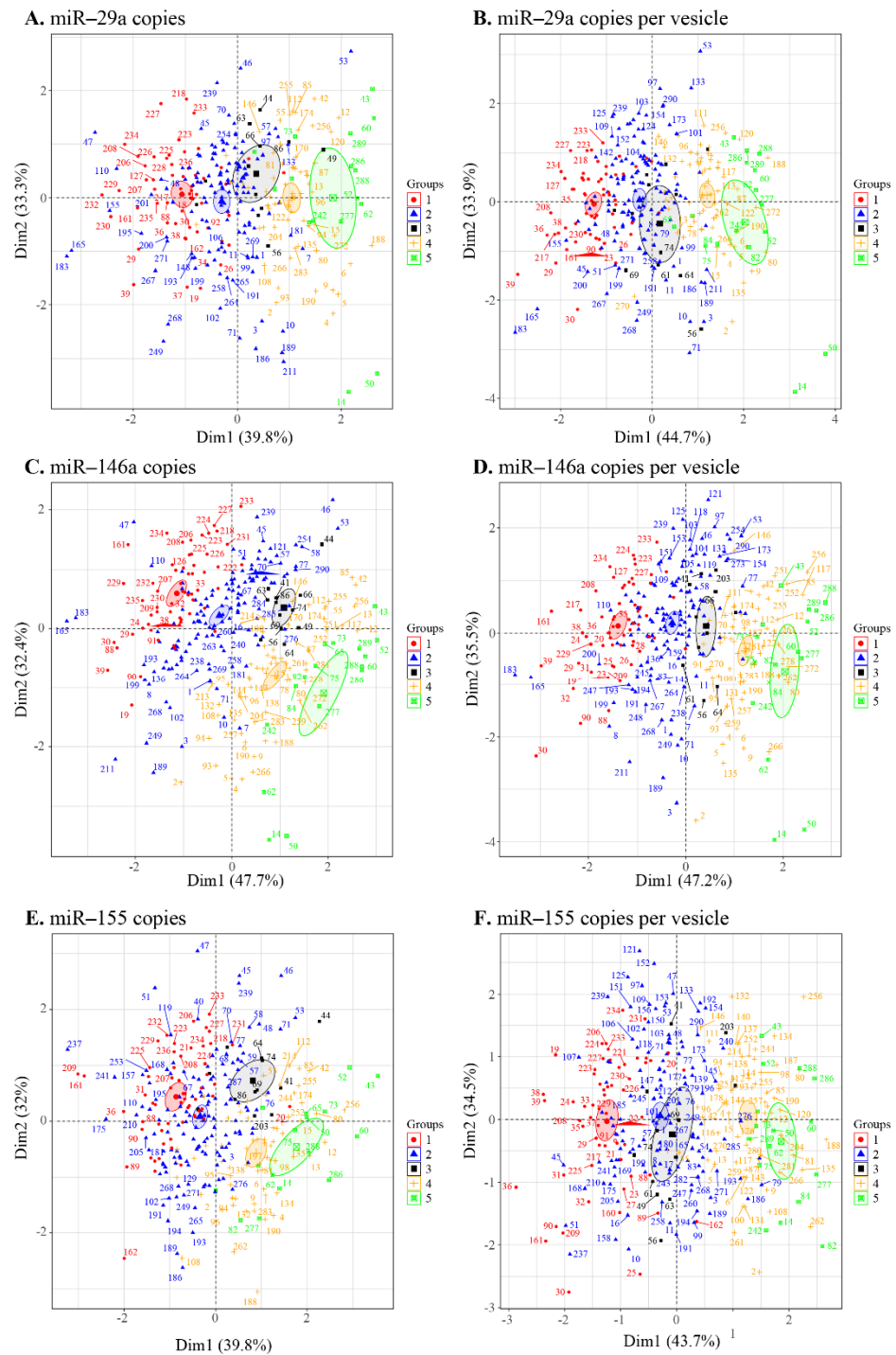


**Figure 6.** Principal component analysis of the microRNA content of large and small EVs in individuals in the five groups ((1) HIV-negative, (2) HIV+ ART-treated nonviremic, (3) HIV+ ART-naïve nonviremic, (4) HIV+ ART-treated viremic, and (5) HIV+ ART-naïve viremic). The miRNAs miR-29a (A), miR-146a (C), and miR-155 (E) contents expressed as copies per  $\mu\text{g}$  of RNA and expressed as copies per vesicle for miR-29a (B), miR-146a (D), and miR-155 (F). Ellipses are drawn around the centroids of the clusters, representing 95% confidence intervals.

**Table 2.** Receiver operating characteristic analysis of EV miRNA content as a discriminator of viremic patients versus control.

	Group Used as Control					
	HIV-Negative		ART-Naïve, Undetectable Viral Load		Reference Patients	
	AUC (95% CI)	p-Value	AUC (95% CI)	p-Value	AUC (95% CI)	p-Value
miR-29a copies, large EVs	0.52 (0.43–0.62)	0.6006	0.63 (0.47–0.78)	0.1548	0.58 (0.38–0.77)	0.4274
miR-29a copies, small EVs	0.71* (0.63–0.80)	<0.0001	0.60 (0.45–0.76)	0.2686	0.50 (0.35–0.65)	0.9600
miR-29a copies per large EV	0.65 (0.56–0.74)	0.0016	0.50 (0.31–0.69)	0.9911	0.54 (0.31–0.76)	0.7099
miR-29a copies per small EV	0.80 (0.73–0.88)	<0.0001	0.88 (0.49–0.97)	<0.0001	0.73 (0.55–0.90)	0.0255
miR-146a copies, large EVs	0.54 (0.44–0.63)	0.4420	0.72* (0.61–0.83)	0.0133	0.60 (0.43–0.78)	0.2914
miR-146a copies, small EVs	0.81 (0.74–0.88)	<0.0001	0.63 (0.52–0.75)	0.1348	0.66 (0.48–0.83)	0.1082
miR-146a copies per large EV	0.56 (0.46–0.65)	0.2285	0.62 (0.45–0.80)	0.1695	0.54 (0.34–0.74)	0.6801
miR-146a copies per small EV	0.89 (0.83–0.94)	<0.0001	0.68 (0.55–0.81)	0.0502	0.77 (0.61–0.93)	0.0054
miR-155 copies, large EVs	0.51 (0.41–0.60)	0.8914	0.80* (0.70–0.90)	0.0007	0.76 (0.63–0.90)	0.0084
miR-155 copies, small EVs	0.63 (0.54–0.72)	0.0093	0.52 (0.35–0.69)	0.8010	0.61 (0.46–0.75)	0.2891
miR-155 copies per large EV	0.68* (0.59–0.77)	0.0002	0.62 (0.45–0.78)	0.1674	0.52 (0.29–0.75)	0.8367
miR-155 copies per small EV	0.76 (0.68–0.85)	<0.0001	0.97 (0.93–1.00)	<0.0001	0.87 (0.77–0.97)	0.0006

HIV: human immunodeficiency virus, ART: antiretroviral therapy, AUC: area under the curve (with 95% confidence interval) based on all viremic patients with  $\geq 20$  copies per mL, and CI: confidence interval. \* Values are higher in the control.

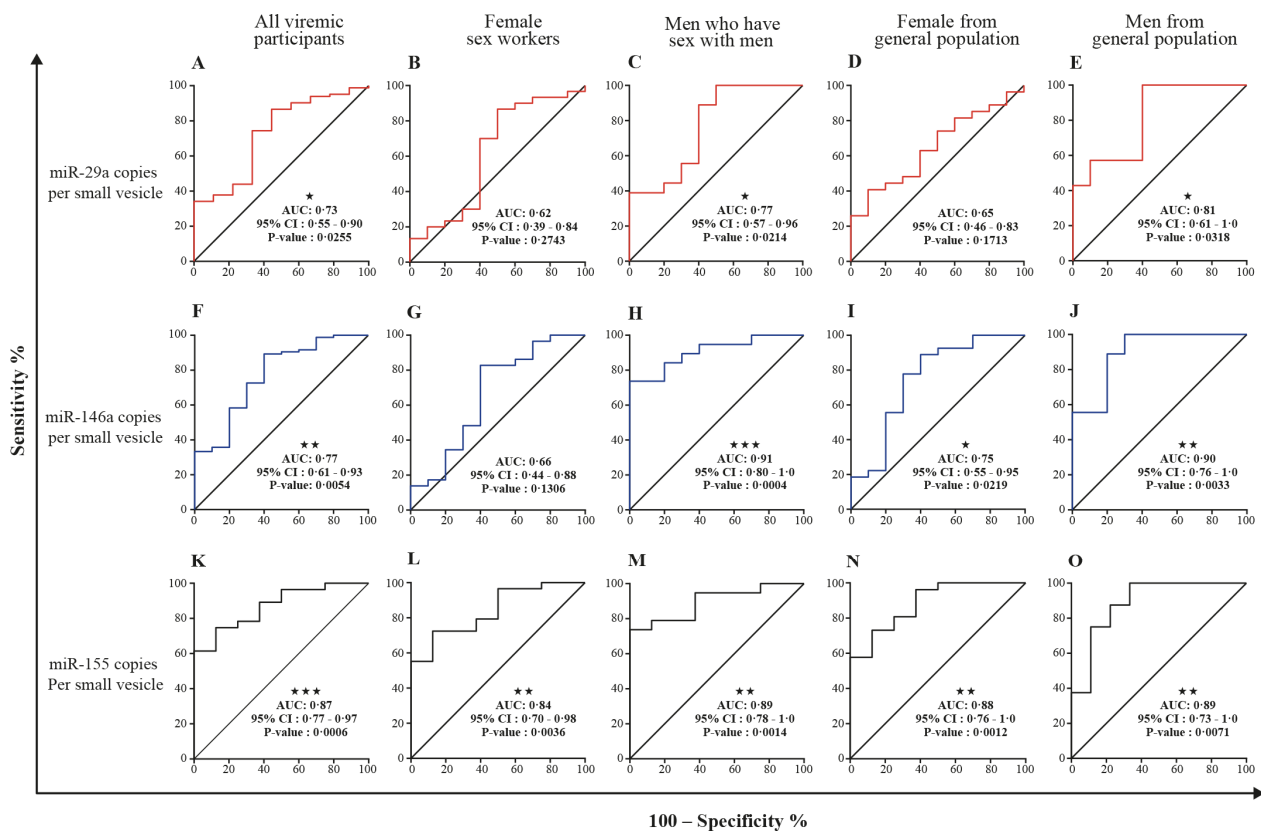


**Figure 7.** Small EV miRNA content diagnosis performances in the receiver operating characteristics curves analysis. MiRNA per small EVs was used to generate a receiver operator characteristic (ROC) curve analysis to discriminate viremic participants in different populations. The nonviremic patients ART-treated for more than six months and having a CD8 T cell count < 500 cells/ $\mu$ L, CD4 T cell count

$\geq 500$  cells/ $\mu\text{L}$ , and  $\text{CD4}/\text{CD8} \geq 1$  (reference patient) as the controls. The diagnosis performance of miRNA expressed as copies per small vesicle for the discrimination of participants with detectable viral loads in all viremic participants were presented for miR-29a (A), miR-146a (F), and miR-155 (K). The diagnosis performance of miRNA expressed as copies per small vesicle for the discrimination of participants with detectable viral loads in female sex worker group participants were presented for miR-29a (B), miR-146a (G), and miR-155 (L). The diagnosis performance of miRNA expressed as copies per small vesicle for the discrimination of participants with detectable viral loads in men who have sex with men were presented for miR-29a (C), miR-146a (H), and miR-155 (M). The diagnosis performance of miRNA expressed as copies per small vesicle for the discrimination of participants with detectable viral loads in female from general population group were presented for miR-29a (D), miR-146a (I), and miR-155 (N). The diagnosis performance of miRNA expressed as copies per small vesicle for the discrimination of participants with detectable viral loads in men from general population group were presented for miR-29a (E), miR-146a (J), and miR-155 (O). Wilson/Brown method was used to compute the area under a ROC curve.

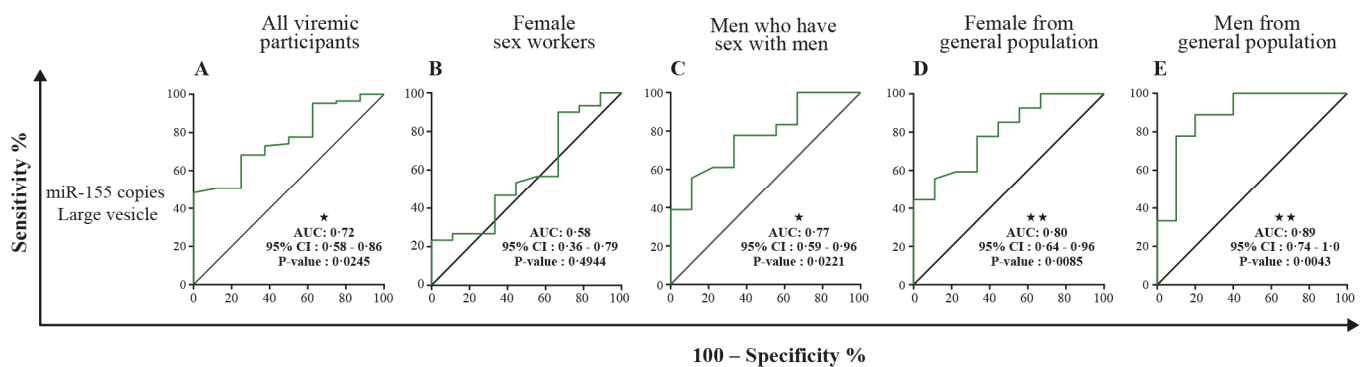


**Figure 8.** Large EV miR-155 content diagnosis performance in the receiver operating characteristics curves analysis. MiR-155 per large EVs was used to generate a receiver operator characteristic (ROC) curve analysis to discriminate viremic participants in different populations. The nonviremic patients ART-treated for more than six months and having a CD8 T cell count  $< 500$  cells/ $\mu\text{L}$ , CD4 T cell count  $\geq 500$  cells/ $\mu\text{L}$ , and  $\text{CD4}/\text{CD8} \geq 1$  (reference patient) undetectable viral load under ART were used as controls. Wilson/Brown method was used to compute the area under a ROC curve. The diagnosis performance of miR-155 copies per  $\mu\text{g}$  of total RNA in large for the discrimination of participants with detectable viral were presented for all participants (A), female sex workers (B), men who have sex with men (C), female from general population (D), and men from general population (E). Wilson/Brown method was used to compute the area under a ROC curve.

#### 4. Discussion

HIV infection alters the physiological state of infected and uninfected cells, both of which release EVs containing substances that reflect the current functional state of the cells. Previous studies have shed light on the role of EVs in HIV-1 pathogenesis, in some cases showing that they prime the body to support the viral spread and that blood EVs reflect tissular activation of specific cell types [19,20]. In this study, two types of plasma EVs and their miRNA contents were evaluated as indicators of viral rebound in ART-treated patients. We found that viral replication is associated with the increased production of large EVs and relatively few small EVs based on flow cytometry. The normal function of EVs as a means of sophisticated intercellular communications for numerous purposes, including signaling the presence of pathogens, can be hijacked by viruses to mediate their propagation, which could explain the increased production of EVs in viremic patients. ART drugs reportedly lower EV secretion by HIV-1-infected cells and alter their content [32]. In addition to targeting different stages of the viral life cycle, ART initially brings some reduction in inflammation and immune activation [33] and could explain the decrease in

EV production. Our results show that small EVs tend to be less abundant in ART-treated patients than in ART-naive patients, viremic or not.

The release of EVs bearing miRNA reportedly regulates the intracellular miRNA levels directly, and EVs may play a role in cell disposal, since they also contain intracellular components that suggest their other use as garbage bags [34,35]. Significant differences in the content of large versus small plasma EVs from HIV+ subjects confirm observations that HIV infection alters the profile of microRNA expression. Our study is one of the first to compare the expression of miR-29a, miR-146a, and miR-155 in viremic and nonviremic patients in association with large and small plasma EVs. We found that miR-29a is overexpressed in small EVs of viremic patients and that its expression per small EV is the best discriminator of ART-treated patients with low viremia. We also found that miR-146a is overexpressed in large and small plasma EVs of persons with detectable viremia. The expression of miR-155 in copies per vesicle appears to be elevated in small EVs and reduced in large EVs in viremic compared to nonviremic patients. Moreover, this expression was the best discriminator of viremic patients.

Although these three miRNAs are known to influence HIV-1 replication *in vitro* in several ways, the quantitative relationship remains unclear, and additional mechanisms might exist. MiR-29a is downregulated during HIV replication and correlates inversely with active HIV-1 replication [23,36]. *In vitro*, it binds to a sequence in the 3'UTR of viral transcripts, silencing viral production and infectivity. Its overexpression downregulates HIV-1 replication and reduces virion infectivity [23,36]. Meanwhile, miR-146a is upregulated in CD4 T-cell-derived EVs from viremic ART-naive HIV+ patients [37]. It is overexpressed in most viral diseases and may be a critical factor in the progression of illness by acting as a brake on the inflammatory response [31]. The relationship between miR-146a and the NF- $\kappa$ B signaling pathway has been reported and is consistent with the involvement of miR-146a in regulating the innate immune response and increased expression in chronic inflammation [31,32,38]. A previous study suggested an increased expression of miR-155 in peripheral blood mononuclear cells and plasma in viremic patients compared to elite controllers or healthy subjects [39]. There is evidence for miR-155 targeting several host-dependent factors involved in post-entry pre-integration events, thereby curtailing HIV-1 infection [38]. MiR-155 has been shown to keep HIV-1 in latency by targeting the TRIM32 transcript and blocking its promotion of HIV-1 reactivation from the latent state [25]. It is also described as a modulator of various aspects and steps of innate and adaptive immune responses [40]. Abundantly expressed in reactivated cells, its expression is required for optimal CD8+ T cell responses to counter viral replication [41,42]. The elevated expression of miR-146 and miR-155 in EVs of viremic patients could serve to inform and protect surrounding cells from HIV infection and help manage host-dependent factors and cellular pathways important for viral replication. The amounts of the three miRNA molecules measured in large and small EVs in this study could be an overall reflection of HIV replication. The reproducibility of our overall results in four subgroups (female sex workers, men who have sex with men, and men and women of the general population) reinforces the biomarker potentials for microRNA in EVs as we monitor ART-treated HIV patients for the earlier detection and management of viral rebound, as illustrated in Figure 9.

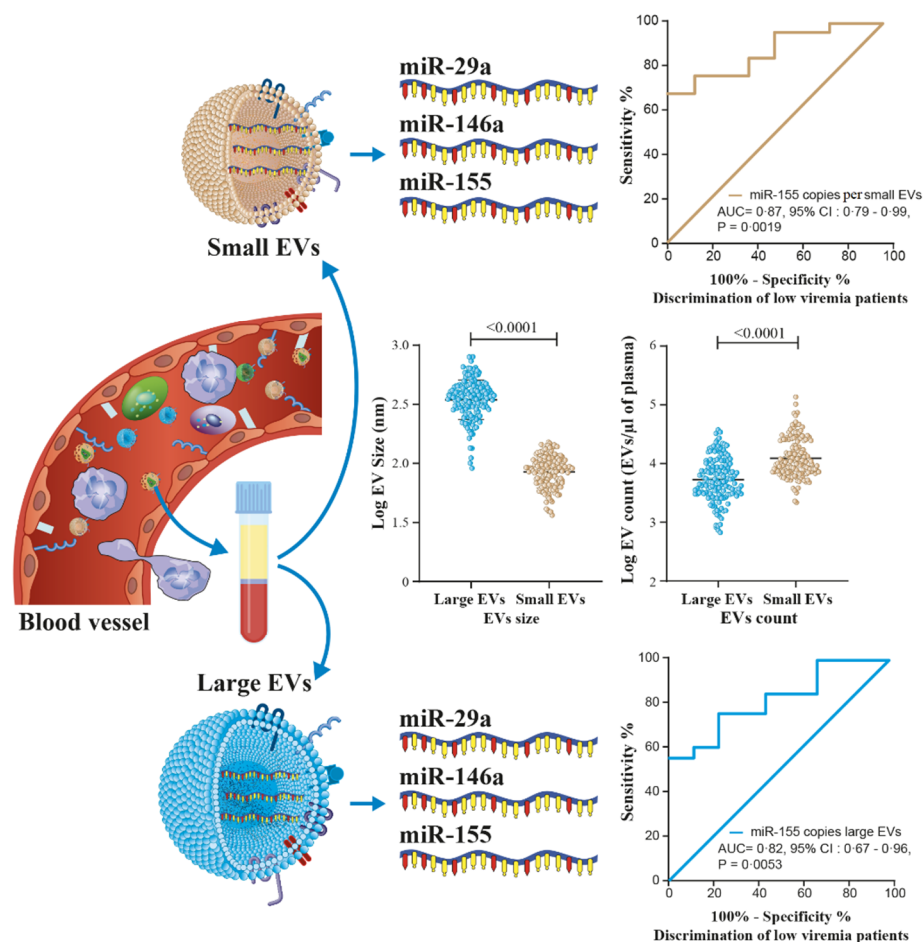


**Figure 9.** Graphical abstract show that microRNA into large or small EVs in plasma from PLWH may be helpful in the prediction of viral rebound as liquid biopsies for different populations.

## 5. Conclusions

In summary, we reported the differential expression of miR-29a, miR-146a, and miR-155 in large and small plasma EVs from viremic and nonviremic, ART-treated and ART-naïve patients and from uninfected persons. The release of EVs from HIV-1-infected cells prior to virion release led us to hypothesize that a clinical analysis of EV contents might provide a biomarker of viral replication in persons living with the virus. We found that miR-29a, miR-146a, and miR-155 expressed as copies per vesicle each discriminate against viremic patients to some extent and could serve this purpose. Due to the cross-sectional nature of our study, a longitudinal follow-up of a cohort of patients is needed to evaluate and validate the suitability of miR-29a, miR-146a, and miR-155 as predictors of viral rebound in ART-treated persons, as well as in an in vitro mechanistic analysis.

**Supplementary Materials:** The following supporting information can be downloaded at <https://www.mdpi.com/article/10.3390/cells11050859/s1>: Table S1: Demographic and clinical characteristics of the study participants. Figure S1: Extracellular vesicles characterization and miRNA content. Figure S2: Extracellular vesicle analysis in cytometry. Figure S3: MicroRNA miR-29a content in large and small EVs linked with the viral load status. Figure S4: MicroRNA miR-146a content in large and small EVs linked with the viral load status. Figure S5: MicroRNA miR-155 content in large and small EVs linked with the viral load status. Figure S6: Correlation matrix between measurements on viremic HIV+ patients, ART-naïve HIV patients with a viral load  $\geq 1000$  copies/mL, ART-treated HIV patients with a viral load  $\geq 1000$  copies/mL, and ART-treated HIV patients with a viral load 20–1000 copies/mL. Table S2: Receiver operating characteristic analysis of the EV miRNA content as discriminant between HIV-negative and viremic patients. Table S3: Receiver operating characteristic analysis of the EV miRNA content as discriminant between nonviremic ART-naïve patients and

viremic patients. Table S4: Receiver operating characteristic analysis of the EV miRNA content as discriminant between reference† patients and viremic patients. Table S5: Receiver operating characteristic analysis of the EV miRNA content as discriminant between HIV-negative and subgroups of viremic patients. Table S6: Receiver operating characteristic analysis of the EV miRNA content as discriminant between nonviremic ART-naïve patients and subgroups of viremic patients. Table S7: Receiver operating characteristic analysis of the EV miRNA content as discriminant between reference† patients and subgroups of viremic patients.

**Author Contributions:** Conceived and designed the experiments: W.W.B. and C.G.; performed the experiments: W.W.B., C.G. and J.B.; analyzed the data: W.W.B. and C.G.; contributed clinical samples, reagents, materials, and analytical tools: W.W.B., I.T.T., D.K., D.Y.S., M.A. and C.G.; and wrote the manuscript: W.W.B. and C.G. All authors have read and agreed to the published version of the manuscript.

**Funding:** The funding sources had no hand in the study design. This research was funded through Canadian Institutes of Health Research (CIHR) grants MOP-188726 and MOP-267056 (HIV/AIDS initiative) to C.G. and the Canadian Institutes of Health Research CIHR Foundation Grant FDN-143218 to M.A. for the studentship awarded to W.W.B. W.W.B. is the recipient of the leadership and sustainable development scholarship and the Fonds de recherche du Québec—Santé (FRQ-S) doctoral training scholarship. W.B.B. and J.B. are recipients of the recruitment scholarship from the AIDS Research Fund of Université Laval and the Desjardins scholarship from the Fondation du CHU de Québec. The FRQ-S supports the Centre de recherche du CHU de Québec—Université Laval infrastructure.

**Institutional Review Board Statement:** This study was conducted in accordance with the Declaration of Helsinki and approved by the Burkina Faso Health Research Ethics Committee (no. 2017-12-182; date 2017-12-20) and the ethics committee of the Centre de Recherche du CHU de Québec-Université Laval, Québec, Canada (Project 2012-890, C12-03-167/Modification F1-32940; date 2018-08-31).

**Informed Consent Statement:** Written informed consent was obtained from all subjects involved in the study.

**Data Availability Statement:** Deidentified participant data from this study and corresponding data dictionary, study protocol, and informed consent documents will be made available to researchers upon request to the corresponding authors. Researchers will be asked to complete a concept sheet for their proposed analyses to be reviewed, and the investigators will consider the overlap of the proposed project with active or planned analyses and the appropriateness of the study data for the proposed analysis.

**Acknowledgments:** The authors thank Stephen Davids for his assistance in editing this manuscript and Martin Pelletier and Stephane Gobeil for access to the qPCR platform. We acknowledge the Bioimaging and cytometry platforms funded by an equipment and infrastructure grant from the Canadian Foundation for Innovation (CFI), Julie-Christine Levesque for microscopy analysis, and Benjamin Goyer for the cytometry analysis. We gratefully acknowledge the continuing collaboration of persons living with HIV. We are particularly grateful to the people of the patient monitoring centers, who allowed and facilitated the recruitment, sample collection, and analysis: Joseph Drabo and Martin Bazongo from CHU Yalgado Ouédraogo day hospital; Elias Dah from the AAS Center; Armel Poda, Abdoul Salam Ouédraogo and Leonel Haltolna from CHU Souro Sanou day hospital; Yacouba Sourabié and Abdoulaye Semde from the immunology service of the CHU-Souro Sanou, Ousseni Bandaogo; Viviane Nikiema from the virology laboratory of the Centre Muraz, Yago Aziz; and Yvette Zoundi and Karambiri Zakaria from Yerelon clinics. Thanks for your help.

**Conflicts of Interest:** The authors declare no conflict of interest.

## References

1. Pierson, T.; McArthur, J.; Siliciano, R.F. Reservoirs for HIV-1: Mechanisms for viral persistence in the presence of antiviral immune responses and antiretroviral therapy. *Annu. Rev. Immunol.* **2000**, *18*, 665–708. [[CrossRef](#)]
2. Aamer, H.A.; McClure, J.; Ko, D.; Maenza, J.; Collier, A.C.; Coombs, R.W.; Mullins, J.I.; Frenkel, L.M. Cells producing residual viremia during antiretroviral treatment appear to contribute to rebound viremia following interruption of treatment. *PLoS Pathog.* **2020**, *16*, e1008791. [[CrossRef](#)]

3. Dinoso, J.B.; Kim, S.Y.; Wiegand, A.M.; Palmer, S.E.; Gange, S.J.; Cranmer, L.; O’Shea, A.; Callender, M.; Spivak, A.; Brennan, T.; et al. Treatment intensification does not reduce residual HIV-1 viremia in patients on highly active antiretroviral therapy. *Proc. Natl. Acad. Sci. USA* **2009**, *106*, 9403–9408. [[CrossRef](#)] [[PubMed](#)]
4. Vandenhende, M.A.; Perrier, A.; Bonnet, F.; Lazaro, E.; Cazanave, C.; Reigadas, S.; Chêne, G.; Morlat, P. Risk of virological failure in HIV-1-infected patients experiencing low-level viraemia under active antiretroviral therapy (ANRS C03 cohort study). *Antivir. Ther.* **2015**, *20*, 655–660. [[CrossRef](#)] [[PubMed](#)]
5. Craw, J.A.; Beer, L.; Tie, Y.; Jaenicke, T.; Shouse, R.L.; Prejean, J. Viral Rebound Among Persons With Diagnosed HIV Who Achieved Viral Suppression, United States. *J. Acquir. Immune Defic. Syndr.* **2020**, *84*, 133–140. [[CrossRef](#)]
6. Bernal, E.; Gómez, J.M.; Jarrín, I.; Cano, A.; Muñoz, A.; Alcaraz, A.; Imaz, A.; Iribarren, J.A.; Rivero, M.; Arazo, P.; et al. Low-Level Viremia Is Associated With Clinical Progression in HIV-Infected Patients Receiving Antiretroviral Treatment. *J. Acquir. Immune Defic. Syndr.* **2018**, *78*, 329–337. [[CrossRef](#)]
7. Bing, A.; Hu, Y.; Prague, M.; Hill, A.L.; Li, J.Z.; Bosch, R.J.; De Gruttola, V.; Wang, R. Comparison of empirical and dynamic models for HIV viral load rebound after treatment interruption. *Stat. Commun. Infect. Dis.* **2020**, *12*, 20190021. [[CrossRef](#)] [[PubMed](#)]
8. Conway, J.M.; Perelson, A.S.; Li, J.Z. Predictions of time to HIV viral rebound following ART suspension that incorporate personal biomarkers. *PLoS Comput. Biol.* **2019**, *15*, e1007229. [[CrossRef](#)]
9. Hatano, H.; Jain, V.; Hunt, P.W.; Lee, T.H.; Sinclair, E.; Do, T.D.; Hoh, R.; Martin, J.N.; McCune, J.M.; Hecht, F.; et al. Cell-based measures of viral persistence are associated with immune activation and programmed cell death protein 1 (PD-1)-expressing CD4+ T cells. *J. Infect. Dis.* **2013**, *208*, 50–56. [[CrossRef](#)]
10. van Niel, G.; D’Angelo, G.; Raposo, G. Shedding light on the cell biology of extracellular vesicles. *Nat. Rev. Mol. Cell Biol.* **2018**, *19*, 213–228. [[CrossRef](#)]
11. Raposo, G.; Stoorvogel, W. Extracellular vesicles: Exosomes, microvesicles, and friends. *J. Cell Biol.* **2013**, *200*, 373–383. [[CrossRef](#)] [[PubMed](#)]
12. Tatischeff, I. Current Search through Liquid Biopsy of Effective Biomarkers for Early Cancer Diagnosis into the Rich Cargoes of Extracellular Vesicles. *Int. J. Mol. Sci.* **2021**, *22*, 5674. [[CrossRef](#)] [[PubMed](#)]
13. Poulet, G.; Massias, J.; Taly, V. Liquid Biopsy: General Concepts. *Acta Cytol.* **2019**, *63*, 449–455. [[CrossRef](#)] [[PubMed](#)]
14. Mathai, R.A.; Vidya, R.V.S.; Reddy, B.S.; Thomas, L.; Udupa, K.; Kolesar, J.; Rao, M. Potential Utility of Liquid Biopsy as a Diagnostic and Prognostic Tool for the Assessment of Solid Tumors: Implications in the Precision Oncology. *J. Clin. Med.* **2019**, *8*, 373. [[CrossRef](#)] [[PubMed](#)]
15. Bazié, W.W.; Boucher, J.; Vitry, J.; Goyer, B.; Routy, J.P.; Tremblay, C.; Trottier, S.; Jenabian, M.A.; Provost, P.; Alary, M.; et al. Plasma Extracellular Vesicle Subtypes May be Useful as Potential Biomarkers of Immune Activation in People with HIV. *Pathog. Immun.* **2021**, *6*, 1–28. [[CrossRef](#)] [[PubMed](#)]
16. Bazié, W.W.; Goyer, B.; Boucher, J.; Zhang, Y.; Planas, D.; Chatterjee, D.; Routy, J.P.; Alary, M.; Ancuta, P.; Gilbert, C. Diurnal Variation of Plasma Extracellular Vesicle Is Disrupted in People Living with HIV. *Pathogens* **2021**, *10*, 518. [[CrossRef](#)] [[PubMed](#)]
17. Lee, J.H.; Schierer, S.; Blume, K.; Dindorf, J.; Wittki, S.; Xiang, W.; Ostalecki, C.; Koliha, N.; Wild, S.; Schuler, G.; et al. HIV-Nef and ADAM17-Containing Plasma Extracellular Vesicles Induce and Correlate with Immune Pathogenesis in Chronic HIV Infection. *EBioMedicine* **2016**, *6*, 103–113. [[CrossRef](#)]
18. Kim, Y.; Mensah, G.A.; Al Sharif, S.; Pinto, D.O.; Branscome, H.; Yelamanchili, S.V.; Cowen, M.; Erickson, J.; Khatkar, P.; Mahieux, R.; et al. Extracellular Vesicles from Infected Cells Are Released Prior to Virion Release. *Cells* **2021**, *10*, 781. [[CrossRef](#)]
19. Sadri Nahand, J.; Bokharaei-Salim, F.; Karimzadeh, M.; Moghooei, M.; Karampoor, S.; Mirzaei, H.R.; Tabibzadeh, A.; Jafari, A.; Ghaderi, A.; Asemi, Z.; et al. MicroRNAs and exosomes: Key players in HIV pathogenesis. *HIV Med.* **2020**, *21*, 246–278. [[CrossRef](#)] [[PubMed](#)]
20. Olivetta, E.; Chiozzini, C.; Arenaccio, C.; Manfredi, F.; Ferrantelli, F.; Federico, M. Extracellular vesicle-mediated intercellular communication in HIV-1 infection and its role in the reservoir maintenance. *Cytokine Growth Factor Rev.* **2020**, *51*, 40–48. [[CrossRef](#)] [[PubMed](#)]
21. Egaña-Gorroño, L.; Escribà, T.; Boulanger, N.; Guardo, A.C.; León, A.; Bargalló, M.E.; Garcia, F.; Gatell, J.M.; Plana, M.; Arnedo, M. Differential microRNA expression profile between stimulated PBMCs from HIV-1 infected elite controllers and viremic progressors. *PLoS ONE* **2014**, *9*, e106360. [[CrossRef](#)]
22. Klase, Z.; Houzet, L.; Jeang, K.T. MicroRNAs and HIV-1: Complex interactions. *J. Biol. Chem.* **2012**, *287*, 40884–40890. [[CrossRef](#)] [[PubMed](#)]
23. Nathans, R.; Chu, C.Y.; Serquina, A.K.; Lu, C.C.; Cao, H.; Rana, T.M. Cellular microRNA and P bodies modulate host-HIV-1 interactions. *Mol. Cell* **2009**, *34*, 696–709. [[CrossRef](#)] [[PubMed](#)]
24. Patel, P.; Ansari, M.Y.; Bapat, S.; Thakar, M.; Gangakhedkar, R.; Jameel, S. The microRNA miR-29a is associated with human immunodeficiency virus latency. *Retrovirology* **2014**, *11*, 108. [[CrossRef](#)] [[PubMed](#)]
25. Ruelas, D.S.; Chan, J.K.; Oh, E.; Heidersbach, A.J.; Hebbeler, A.M.; Chavez, L.; Verdin, E.; Rape, M.; Greene, W.C. MicroRNA-155 Reinforces HIV Latency. *J. Biol. Chem.* **2015**, *290*, 13736–13748. [[CrossRef](#)] [[PubMed](#)]
26. Hiroi, T.; Shibayama, M. Measurement of Particle Size Distribution in Turbid Solutions by Dynamic Light Scattering Microscopy. *J. Vis. Exp.* **2017**, *9*, e54885. [[CrossRef](#)] [[PubMed](#)]

27. Van Deun, J.; Mestdagh, P.; Agostinis, P.; Akay, Ö.; Anand, S.; Anckaert, J.; Martinez, Z.A.; Baetens, T.; Beghein, E.; Bertier, L.; et al. EV-TRACK: Transparent reporting and centralizing knowledge in extracellular vesicle research. *Nat. Methods*. **2017**, *14*, 228–232.
28. Mfunyi, C.M.; Vaillancourt, M.; Vitry, J.; Nsimba Batomene, T.R.; Posvandzic, A.; Lambert, A.A.; Gilbert, C. Exosome release following activation of the dendritic cell immunoreceptor: A potential role in HIV-1 pathogenesis. *Virology* **2015**, *484*, 103–112. [[CrossRef](#)]
29. Hubert, A.; Subra, C.; Jenabian, M.A.; Tremblay Labrecque, P.F.; Tremblay, C.; Laffont, B.; Provost, P.; Routy, J.P.; Gilbert, C. Elevated Abundance, Size, and MicroRNA Content of Plasma Extracellular Vesicles in Viremic HIV-1+ Patients: Correlations With Known Markers of Disease Progression. *J. Acquir. Immune Defic. Syndr.* **2015**, *70*, 219–227. [[CrossRef](#)]
30. Taganov, K.D.; Boldin, M.P.; Chang, K.J.; Baltimore, D. NF-kappaB-dependent induction of microRNA miR-146, an inhibitor targeted to signaling proteins of innate immune responses. *Proc. Natl. Acad. Sci. USA* **2006**, *103*, 12481–12486. [[CrossRef](#)] [[PubMed](#)]
31. Nahand, J.S.; Karimzadeh, M.R.; Nezamnia, M.; Fatemipour, M.; Khatami, A.; Jamshidi, S.; Moghoofei, M.; Taghizadieh, M.; Hajighadimi, S.; Shafiee, A.; et al. The role of miR-146a in viral infection. *IUBMB Life* **2020**, *72*, 343–360. [[CrossRef](#)] [[PubMed](#)]
32. DeMarino, C.; Pleet, M.L.; Cowen, M.; Barclay, R.A.; Akpamagbo, Y.; Erickson, J.; Ndembu, N.; Charurat, M.; Jumare, J.; Bwala, S.; et al. Antiretroviral Drugs Alter the Content of Extracellular Vesicles from HIV-1-Infected Cells. *Sci. Rep.* **2018**, *8*, 7653. [[CrossRef](#)] [[PubMed](#)]
33. Hileman, C.O.; Funderburg, N.T. Inflammation, Immune Activation, and Antiretroviral Therapy in HIV. *Curr. HIV/AIDS Rep.* **2017**, *14*, 93–100. [[CrossRef](#)]
34. Hessvik, N.P.; Llorente, A. Current knowledge on exosome biogenesis and release. *Cell. Mol. Life Sci.* **2018**, *75*, 193–208. [[CrossRef](#)]
35. Baixauli, F.; López-Otín, C.; Mittelbrunn, M. Exosomes and autophagy: Coordinated mechanisms for the maintenance of cellular fitness. *Front. Immunol.* **2014**, *5*, 403. [[CrossRef](#)] [[PubMed](#)]
36. Ahluwalia, J.K.; Khan, S.Z.; Soni, K.; Rawat, P.; Gupta, A.; Hariharan, M.; Scaria, V.; Lalwani, M.; Pillai, B.; Mitra, D.; et al. Human cellular microRNA hsa-miR-29a interferes with viral nef protein expression and HIV-1 replication. *Retrovirology*. **2008**, *5*, 117. [[CrossRef](#)]
37. Balducci, E.; Leroyer, A.S.; Lacroix, R.; Robert, S.; Todorova, D.; Simoncini, S.; Lyonnet, L.; Chareyre, C.; Zaegel-Faucher, O.; Micallef, J.; et al. Extracellular vesicles from T cells overexpress miR-146b-5p in HIV-1 infection and repress endothelial activation. *Sci Rep.* **2019**, *9*, 10299. [[CrossRef](#)]
38. Swaminathan, G.; Rossi, F.; Sierra, L.J.; Gupta, A.; Navas-Martín, S.; Martín-García, J. A role for microRNA-155 modulation in the anti-HIV-1 effects of Toll-like receptor 3 stimulation in macrophages. *PLoS Pathog.* **2012**, *8*, e1002937. [[CrossRef](#)]
39. Witwer, K.W.; Watson, A.K.; Blankson, J.N.; Clements, J.E. Relationships of PBMC microRNA expression, plasma viral load, and CD4+ T-cell count in HIV-1-infected elite suppressors and viremic patients. *Retrovirology* **2012**, *9*, 5. [[CrossRef](#)]
40. Elton, T.S.; Selemon, H.; Elton, S.M.; Parinandi, N.L. Regulation of the MIR155 host gene in physiological and pathological processes. *Gene* **2013**, *532*, 1–12. [[CrossRef](#)]
41. Jin, C.; Cheng, L.; Lu, X.; Xie, T.; Wu, H.; Wu, N. Elevated expression of miR-155 is associated with the differentiation of CD8+ T cells in patients with HIV-1. *Mol. Med. Rep.* **2017**, *16*, 1584–1589. [[CrossRef](#)] [[PubMed](#)]
42. Lind, E.F.; Elford, A.R.; Ohashi, P.S. Micro-RNA 155 is required for optimal CD8+ T cell responses to acute viral and intracellular bacterial challenges. *J. Immunol.* **2013**, *190*, 1210–1216. [[CrossRef](#)] [[PubMed](#)]